Journal of Alloys and Compounds 489 (2010) 20–25

Contents lists available at ScienceDirect

Journal of Alloys and Compounds

journal homepage: www.elsevier.com/locate/jallcom

An approach for obtaining the structural diversity of multi-walled carbon nanotubes on Ni/Al catalyst with low Ni content

C.N. He, N.Q. Zhao*, C.S. Shi, S.Z. Song

School of Materials Science and Engineering, Tianjin University, Tianjin 300072, China

ARTICLE INFO

Article history:
Received 20 April 2009
Received in revised form 24 August 2009
Accepted 15 September 2009
Available online 23 September 2009

Keywords:
Nanomaterials
Catalysts
Chemical vapor deposition
Bamboo-shaped

ABSTRACT

A mass of multi-walled carbon nanotubes were fabricated on Ni/Al catalyst with low Ni content (2.5 wt.%) by chemical vapor deposition in the temperature range of 773–923 K and characterized with respect to their structure. The tubular and the bamboo-shaped structure occurred in the 773–873 K and 873–923 K temperature ranges, respectively. In order to figure out the reasons for the observed structural instabilities, the effects of reduction and reaction temperature on the catalyst particle sizes and the carbon nanotube dimensions (lengths and diameters) were investigated in detail using statistical measurements based on transmission electron microscope observations. The reduction and reaction temperatures have strong influences on the catalyst particle sizes and the carbon nanotube diameters. The influence of reaction temperatures on the carbon nanotube length is feeble. Furthermore, mechanisms of the structure formation are discussed as well as open questions are addressed.

1. Introduction

Carbon nanotubes (CNTs) have attracted much attention due to unique tubular structure and abundant physical and chemical properties. Recently, CNTs with special structures such as bamboo-shaped [1,2], octopus [3], fish-bone [4], and coils [5], which are different from the conventional straight tubes, have attracted immense interest from scientists around the world. As the most common member of this family, bamboo-shaped CNTs, consisting of many separated hollow compartments, have been frequently investigated to explore their unique structure-associated properties and to understand the relationship between their formation and the growth of conventional straight tubes that exhibit continuous hollow channels. At the same time, exploring the appropriate growth conditions for bamboo-shaped nanotubes versus conventional straight nanotubes can also induce their controllable synthesis and modify their structures selectively.

To date, bamboo-shaped CNTs can be fabricated through various methods such as arc-discharge, pyrolysis of organometallic compounds, and chemical vapor deposition (CVD) [6–9]. CNT growth by CVD is both efficient and versatile and, therefore, the technologically most relevant process for the synthesis of this interesting nanomaterial attracts much attention. CVD growth of CNTs from hydrocarbon precursor molecules is facilitated by the catalytic activity of transition metal particles at elevated temperatures with diameters in the nanometer range. Well dispersed carrier-supported catalyst particles are employed for the synthesis of CNTs. Identification and control of critical growth parameters is crucial for process optimization and development of CNT growth mechanism. Besides growth temperature and chemical properties of precursor and catalysts, the catalyst particle size, to a large degree, is believed to control the CNT diameter [10,11]. It is known that the properties of CNTs depend strongly on their chiralities [12]. In turn, the chirality is determined by the CNT diameter and the orientation of the rolled graphene sheet with respect to the CNT axis. Hence, control of the catalyst size is an important step towards the properties of CNTs, and various studies on the preparation of size-controlled transition metal catalyst particles for CNT growth have been carried out [13–15].

Previously, we have obtained a mass of bamboo-shaped CNTs in the process of catalytic decomposition of methane over Ni/Al catalyst with relatively high Ni content [16]. We have since paid much attention to this interesting nanostructure, because the systematical experiments are very beneficial for the comprehension of growth mechanism, and as well for the controllable synthesis of bamboo-shaped CNTs. However, a lack of knowledge concerns the relationships between catalyst particles size, structure of the CNT and growth conditions. According to the experimental findings and known facts, we try to figure out some of the reason for the occurrence of different structures of CNTs synthesized on Ni/Al catalyst with low Ni content, which is the focus of the current paper.

* Corresponding author. Tel.: +86 22 87401601; fax: +86 22 27405874.
E-mail address: nqzhao@tju.edu.cn (N.Q. Zhao).

0925-8388/$ – see front matter © 2009 Elsevier B.V. All rights reserved.
doi:10.1016/j.jallcom.2009.09.067

2. Experimental

2.1. Preparation of the catalyst

The catalyst precursor of $Ni(OH)_2$/Al was fabricated using a deposition–precipitation route [16,17]. For the deposition–precipitation process, the right amounts of $Ni(NO_3)_2{\cdot}6H_2O$ (0.01 mol) and aluminum powder (0.85 mol) were mixed in 1 l distilled water, then appropriate NaOH solution was added to the previous mixture with constant stirring to obtain the binary colloid ($Ni(OH)_2$/Al). The colloid obtained was washed several times with distilled water till neutral pH and dried in a vacuum drying chamber at 393 K for 6 h. Ultimately the colloid was calcined at 473 K for 4 h in N_2 to form fine NiO/Al powder, which was employed in the following catalytic synthesis experiments. Reagent grade $Ni(NO_3)_2{\cdot}6H_2O$, reagent grade aluminum powder and reagent grade NaOH were obtained from Tianjin Chemical Reagent Company.

2.2. Synthesis of the CNTs

To synthesize the CNTs, approximately 400 mg NiO/Al powder was sprayed uniformly into a quartz boat, which was inserted into a tube furnace. The tube furnace was heated to a reduction temperature of 673 K under N_2. Then N_2 valve was closed and H_2 (200 ml/min, 99.99% purity) was introduced to reduce the NiO/Al for 2 h. Subsequently, shut off the H_2 flow, and a mixture of $CH_4/N_2/H_2$ (60 ml/min/480 ml/min/120 ml/min, v/v/v, 99.99% purity/99.99% purity/99.99% purity) was introduced into the furnace with a flow rate of 660 ml/min. Finally, the sample was maintained at the reaction temperature (773 K, 823 K, 873 K, 893 K, 903 K and 923 K) for 1 h and six samples were thus obtained, which were indicated as S1, S2, . . ., S5 and S6, respectively.

In order to characterize the Ni/Al catalyst by transmission electron microscope and X-ray diffractometer, the NiO/Al powder was reduced to Ni/Al in H_2 for 2 h at various temperatures (673 K, 723 K, 823 K or 873 K). After the reduction step, the samples were cooled down to room temperature under the flow of N_2/H_2 to prevent the oxidation of the Ni nanoparticles.

2.3. Characterization techniques

The morphology and microstructure of the catalyst and the CNTs have been investigated using a high-resolution transmission electron microscope (HRTEM) (PHILIPS TECNAI G^2 F20). In order to analyze the component, the catalysts before and after reduction were characterized by using a Rigaku D/max 2500V/pc automated X-ray diffractometer (XRD) with Cu Kα radiation. The error of the dimension measurements is determined by the TEM scale bar calibrations and a ruler gradation (1 mm). The scale bar of the TEM was calibrated conventionally with the help of the crystalline silicon standard on the basis of its known crystallographic data, i.e., lattice parameters. The maximum absolute error that can appear from the dimension measurements is about 0.2 nm. Number distributions of Ni nanoparticle diameters and CNT dimensions (diameters and lengths) were measured manually on the basis of high-resolution TEM images. The number of measurements for each dimension and for each case was about 100. Raman of S5 sample was performed using Bruker RFS 100/S.

3. Results and discussions

3.1. Characterization of the catalyst

Fig. 1(a) shows the XRD patterns of the catalyst precursor of NiO/Al powder (curve a) and the typical catalyst reduced at 673 K for 2 h (curve b). From curve a in Fig. 1(a), we can observe the strong aluminum peaks and the feeble NiO peaks. The pattern of the reduced catalyst is shown in curve b of Fig. 1(a). It can be seen that the NiO peaks disappeared instead of the Ni peaks appearing, indicating that the NiO has been completely reduced to Ni after reduction. Fig. 1(b) shows the distribution of a typical catalyst particles obtained by the reduction of the NiO/Al in H_2 at 673 K for 2 h. As can be seen, uniform and small (10–20 nm) nickel nanoparticles disperse on the Al surfaces, which are very beneficial for production of CNTs with a narrow distribution of diameters.

Number distributions of diameters of catalyst particles reduced at various temperatures from 673 K to 873 K were measured manually on the basis of HRTEM images. The number of measurements was 100. Since the diameters were better described by log-normal distributions, the geometric mean diameter was calculated as

$$\lg D_g = \frac{\sum n_i \lg D_i}{N} \quad (1)$$

where n_i is the number of catalyst particles with a diameter of D_i, N is a number of measurements. A standard geometric deviation can be found as

$$\lg \sigma = \left[\frac{\sum n_i(\lg D_i - \lg D_g)^2}{N-1}\right]^{1/2} \quad (2)$$

The reduction temperature, which is the only source of energy in the reduction of the catalyst, is of great importance in order to achieve uniform diameter distribution for the active Ni nanoparticles. To investigate the effect of reduction temperature on the diameter of the nickel particles, we reduced the catalyst precursor of NiO/Al at various temperatures (673 K, 823 K, 673 K and 873 K), while fixing the other conditions (reduction time of 2 h, 200 ml/min of H_2). Fig. 2(a) shows the number diameter distributions of the catalytic particles. Increasing the reduction temperature from 673 K to 873 K leads to an increase in the geometric mean diameter of the catalytic particles from 11 nm to 15.8 nm (with the geometric standard deviations of about 1.53). The increase in the diameter of

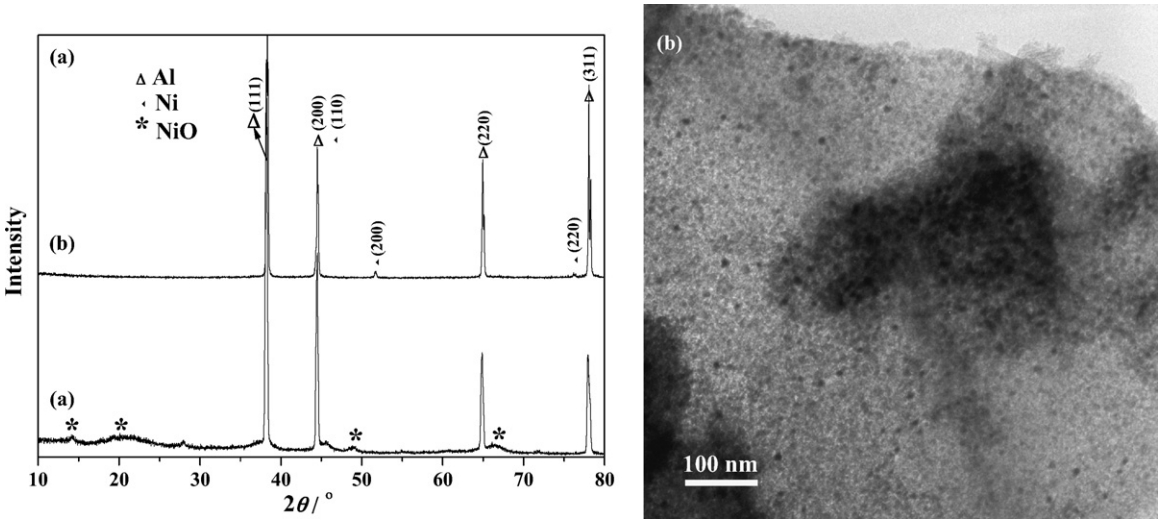

Fig. 1. (a) XRD patterns of catalyst sample before reduction (curve a) and after reduction at 673 K (curve b) and (b) TEM image of the catalyst reduced at 673 K in hydrogen for 2 h.

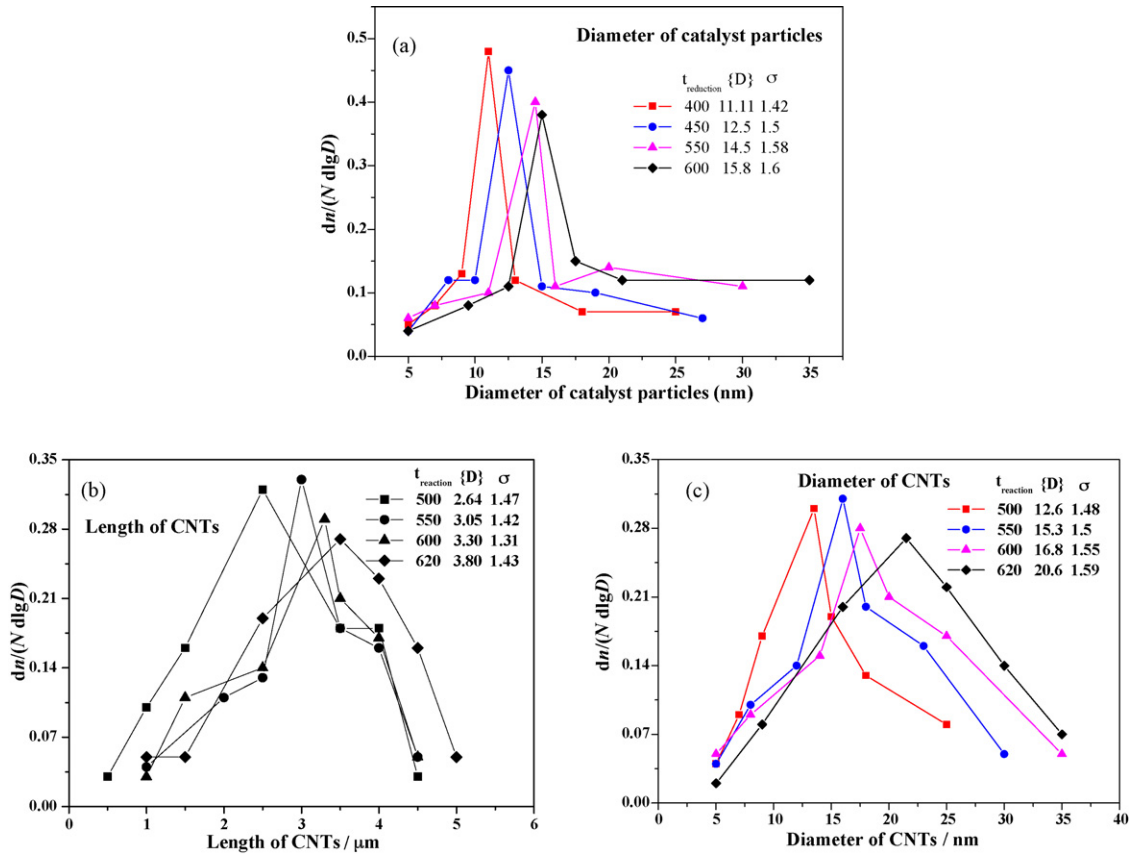

Fig. 2. (a) Number distributions of diameters of catalyst particles reduced at various temperatures when the reduction time equals to a constant of 2 h. Number distributions of (b) lengths and (c) diameters of CNTs synthesized at various temperatures.

the catalytic particles is due to agglomeration or sintering of the catalyst nanoparticles during reduction. As reduction temperature increases, the catalyst nanoparticles are expected to more easily agglomerate and become larger.

3.2. Characterization of the bamboo-shaped CNTs

Number distributions of CNT dimensions (lengths and diameters) were also measured manually on the basis of TEM images. The number of measurements for each dimension and for each case was 100. The geometric mean dimensions (length and diameter) of the CNTs were also calculated using Eq. (1), where n_i is the number of CNTs with a dimension of D_i, N is a number of measurements. A standard geometric deviation can also be found using Eq. (2).

Number distributions of lengths and diameters of the CNTs fabricated at various temperatures are presented in Fig. 2(b) and (c). Fig. 2(b) shows the number length distributions of the CNTs. It can be seen that the geometric mean length of CNTs increases from 2.64 μm to 3.8 μm (with the geometric standard deviations of about 1.41) while increasing the reaction temperature from 773 K to 893 K. The reaction temperature has a stronger influence on diameters of CNT than on the lengths of the CNTs. Fig. 2(c) shows number diameter distributions of the produced CNTs. The geometric mean diameter of CNTs varies from 12.6 nm to 20.6 nm (with the geometric standard deviation between 1.48 and 1.59) as the reaction temperature is increased from 773 K to 893 K.

TEM study on CNTs was also carried out to investigate the effect of synthesis temperature on the structural characteristics of CNTs. We checked several hundreds of individual CNTs and found them all multilayer structure. Fig. 3 shows the TEM images of a few typical CNTs fabricated at 773–923 K. It can be seen that all samples have a mass of crooked and entangled fibers, which are with hollow and multi-walled tube structure. Furthermore, every CNT has a catalyst particle at one end, and the other end is closed, indicating that the diameter of the CNTs is decided by metal catalyst size. A majority of CNTs are well-graphited and with a small curvature, but a few CNTs have a big curvature (>90°) and generate continuous variations in their bend positions, which indicates that Stone–Wales distortion occurs in these CNTs. Though the sections of these CNTs have prodigious distortion, these CNTs maintain intact, indicating that these CNTs have excellent flexibility and are suitable for reinforcing composites.

Fig. 3(a) is a typical TEM image of the CNTs fabricated at 773 K. It can be observed that the CNT yield is low and many amorphous carbon impurities are presented in the sample. The CNT surfaces are very coarse due to impurities attached, and the length and diameter of the CNTs all are small (shown in Fig. 2(b) and (c)). When the reaction temperature increases to 873 K and 903 K, as can be seen in Fig. 3(b) and (c), respectively, the as-obtained samples have few impurities and are with high purity (the CNT purity is estimated to be higher than 96% according to TEM observations). The length of the CNTs is relatively long and their walls are very clean. When the reaction temperature increases to 923 K, the production has very few CNTs and a mass of amorphous carbon impurities exist in the sample. Above experimental evidences are attributed to transformation of the catalyst morphology as temperature increases. At low temperature (such as 773 K), the catalytic activity of the catalyst is relatively low to develop CNT growth, thus a mass of carbon atoms decomposed from methane were deposited around catalytic particles. At too high temperatures (such as 923 K), the catalyst becomes highly mobile and quickly agglomerates into metal particles that are too large to initiate CNT nucleation, on the other hand, the high

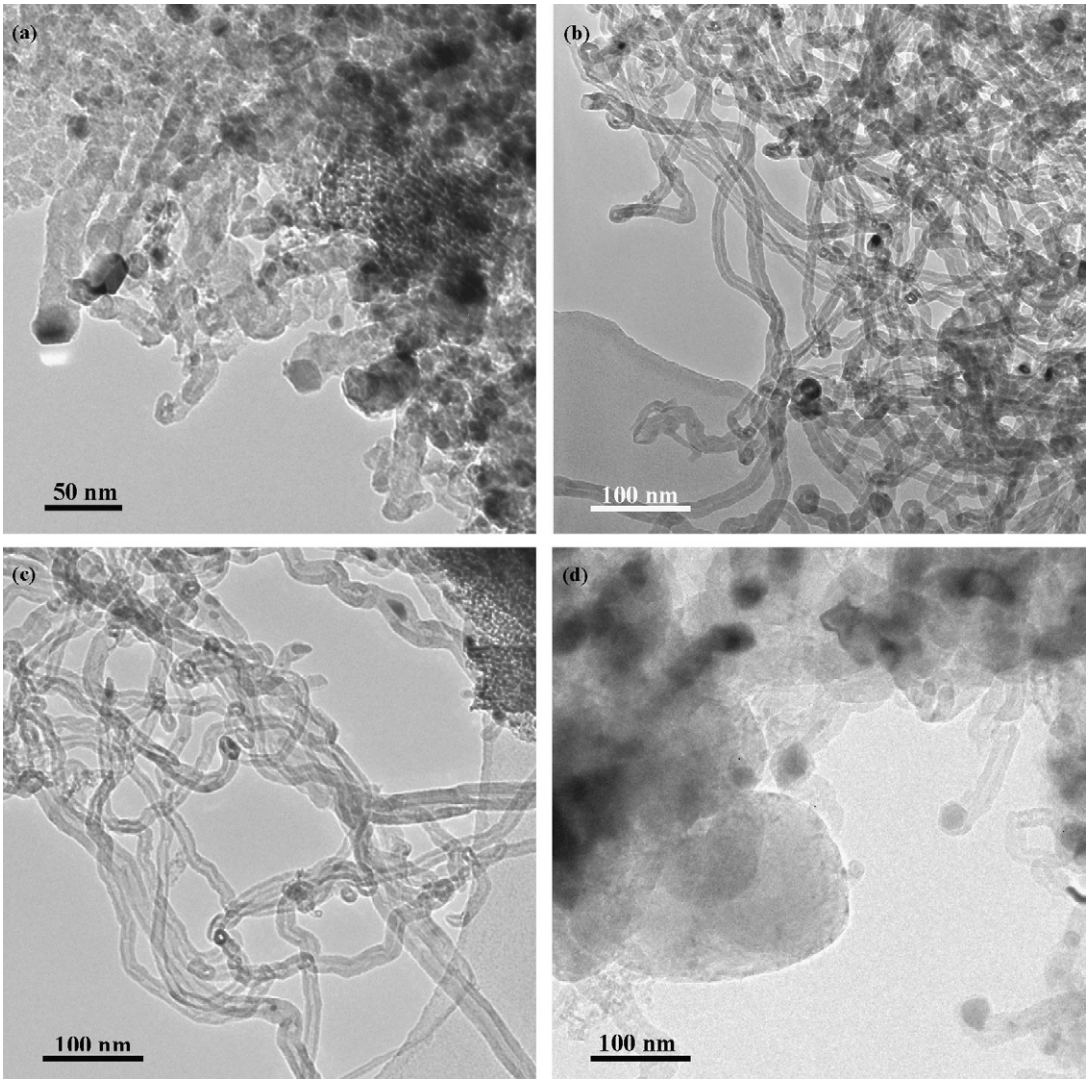

Fig. 3. TEM images of the CNTs synthesized at various reaction temperatures: (a) 773 K, (b) 873 K, (c) 903 K and (d) 923 K.

temperature (such as 923 K), which is close to the melting temperature of Al, easily leads to the melt of catalyst supporter (Al) and thus makes the catalytic particles inactive.

Furthermore, it is observed from the HRTEM micrographs that the hollowness and structure of CNTs and the geometry of catalyst particles are affected by synthesis temperature. For the CNTs synthesized at 773 K and 823 K (as shown in Fig. 4(a) and (b)), the hollowness is not very apparent and the CNTs are with bamboo-shaped structure. The graphite sheets are tilted against the tube axis and they terminate at the outer tube wall. They can also terminate at the inner hollow core (see arrows in Fig. 4(a)) forming open stacked cones, or they form closed stacked cones, which are manifested by bridges of graphite layers inside the hollow core. The distance between the bridges may be caused by the stacked open cones. At the absence of open cones, a displacement of the catalyst particles from the carbon bridges could be explained by continued growth of the cone side walls after the delamination of the carbon bridges from the tip of the catalyst particle. This assumes that the growth of the cones starts at the tip region of the particles and, that different rates for the bridge formation and the growth of the carbon side walls control the formation of the closed carbon cones. Furthermore, a different inclination of the cone side walls and the faces of the catalyst particles has to be presumed for geometrical reasons. For the CNTs synthesized at 873 K, 893 K and 903 K, they have relatively larger hollowness and are with straight tubular structure. The graphite layers are arranged parallel to the tube axis and the catalyst particles at the top of tubes are spherically shaped or form droplets.

The growth mechanism of carbon nanofibers on Ni catalyst has been studied extensively [18–24]. According to Baker et al. [18,19], decomposition of acetylene on a Ni metal substrate and carbon dissolution into Ni metal, followed by carbon diffusion and precipitation are repeated for the growth of carbon filaments. Recently Helveg et al. [22] suggested that the growth mechanism depends on surface diffusion of carbon and nickel atoms through the observation of the in situ transmission electron microscopy. Gozzi et al. [23,24] have investigated the thermodynamic quantities associated with the CVD synthesis from a light hydrocarbon of CNTs and obtained a whole picture of the thermodynamics of this reaction as function of temperature has been obtained. But above results do not necessarily exclude the Backer model and we will discuss the growth mechanism on the basis of the Backer model. In the Backer model, the carbon containing compounds are decomposed on the surface of the catalyst particles and, that adsorbed carbon is dissolved in the particles forming a supersaturated solution followed by precipitation of graphite. The tube growth is sustained via diffusion of carbon through the catalyst particles. Even if not always clearly stated, this model assumes the catalyst particles being in

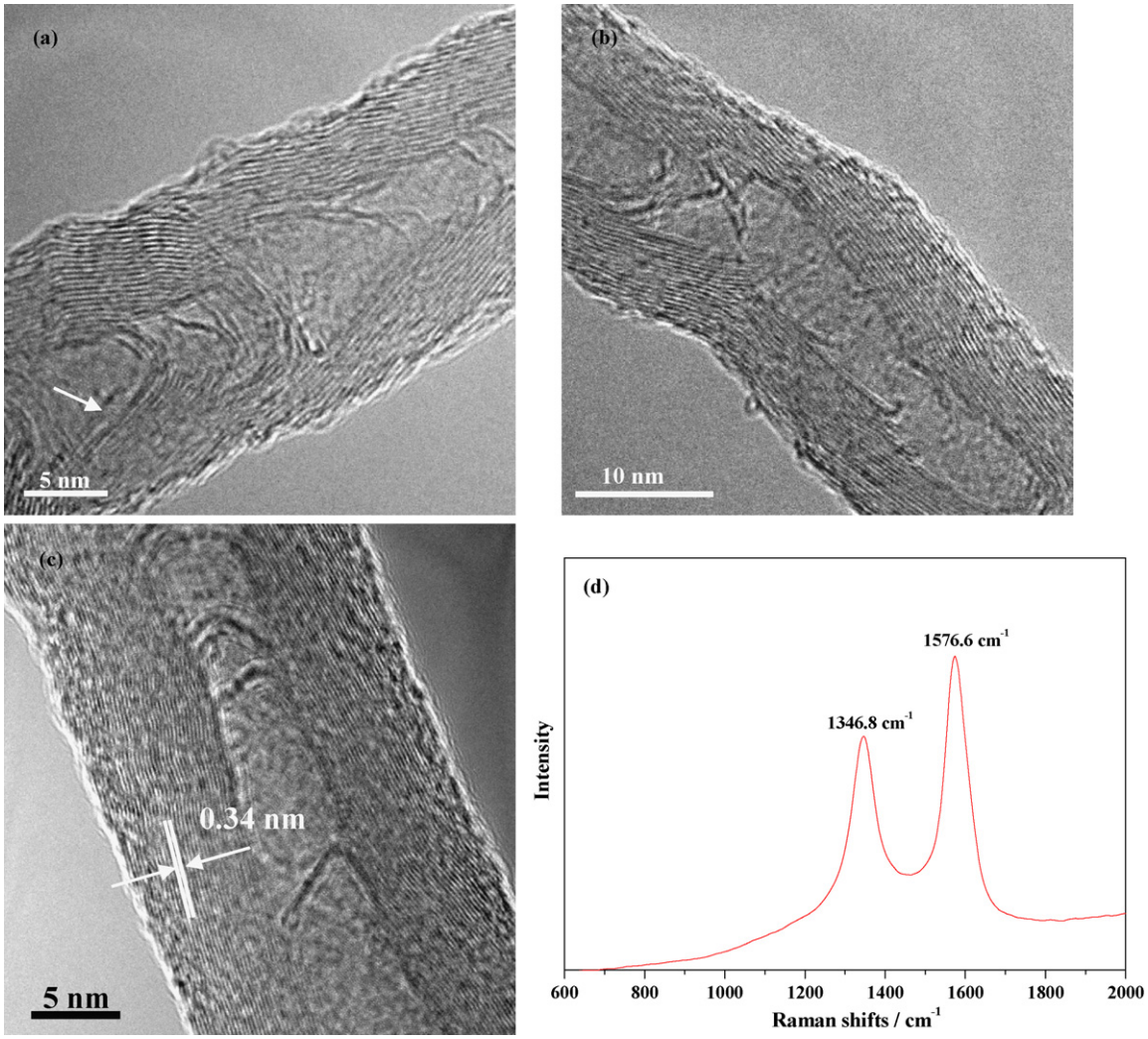

Fig. 4. HRTEM images of the CNTs synthesized at various reaction temperatures: (a) 773 K, (b) 823 K, (c) 903 K and (d) Raman spectrum of CNT sample fabricated at 903 K.

a metastable state in any case. The state of the particles seems to control the basic structure of the formed multi-walled CNT.

In the case of the bamboo-shaped structure obtained at 773 K and 823 K, the catalyst particles during CNT synthesis are in solid state due to low synthesis temperature. For energetic reasons (highest carbon activity) the nucleation of carbon can be expected to start at regions with the highest curvature, it means at the tips of the cone shaped particles. The reasons for forming a closed or an open cone are not clear. According to Terrones et al. [25], the formation of closed cones requires the introduction of pentagonal carbon rings, whereas open cones offer more possibilities of graphitic geometries such as the great variety of chiral configurations.

For the tubular structure obtained at higher temperatures of 873 K, 903 K and 923 K, the spherical shape of the particles makes probable a molten particle state during the growth. Melting of particles at temperatures some hundreds degree below the eutectic temperature of the catalyst metal–carbon alloys (e.g. T_{eut}(Ni) = 1587 K) is explained by the high surface to volume ratio of the nanoparticles [26]. It is well known that the melting temperature of small particles can be significantly reduced by decreasing the particle size [27]. A similar sensitivity to particle size is observed, for example, for solubility. Thus, the macroscopic properties are not strictly applicable to nanometer-sized particles and it is likely that, even at temperatures below 1587 K, there is significant dissolution of carbon in molten metal particles. The nucleation step of the formation of the tubular structure is still not well understood. The contact area between the catalyst particle and the substrate could be crucial for the nucleation. There is experimental indication that the growth may start in this region forming a cap which is the base of growing tube shells. This suggestion implies the formation of the subsequent inner graphitic caps to be favored by the metal–graphite interface.

The as-obtained carbon sample (S5) was also characterized by Raman spectroscopy in detail to validate the presence of CNTs. A representative Raman spectrum (Fig. 4(d)) of the composite powders exhibits two peaks (1346.8 cm^{-1} and 1576.6 cm^{-1}) corresponding to multi-walled CNTs, which are associated with the vibrations of carbon atoms with dangling bonds for the in-plane terminations of disordered graphite (D), and the vibrations in all sp^2-bonded carbon atoms in a 2D hexagonal lattice (G), respectively [28,29]. The intensity ratio of the D band to the G band (corresponding to the vibrations) (I_D/I_G) was calculated to be 0.76. The low relative intensity of the D band peak implies that the obtained CNTs are mainly composed of well-crystallized graphite, which is in agreement with the HRTEM observations.

4. Conclusions

A mass of multi-walled carbon nanotubes (CNTs) were fabricated on Ni/Al catalyst with low Ni content (2.5 wt.%) by chemical

vapor deposition in the temperature range of 773–923 K. The tubular and the bamboo-shaped structure occurred in the 773–873 K and 873–923 K temperature ranges, respectively. It was found that the reduction and reaction temperatures have strong influences on the catalyst particle sizes and the CNT diameters. The influence of reaction temperatures on the CNT length is feeble. The production of multi-walled CNT on catalyst layers by chemical vapor deposition is mainly governed by the metastable state of the catalyst particles, which is related to the particle size, the deposition temperature, and the deposition time. The growth on liquid particles yields tubular multi-walled CNT of smaller diameters, whereas bamboo-shaped tubes with larger diameters are formed on solid particles. Due to the size distribution of the particles, formed at the beginning of the processes, the occurrence of different structures is to be expected for synthesis temperatures high enough to achieve a reasonable structure formation.

Acknowledgements

The authors acknowledge the financial support by National Natural Science Foundation of China (No. 50771071) and Postdoctoral Science Foundation of China (No. 20080440098).

References

[1] Y. Saito, T. Yoshikawa, J. Cryst. Growth 134 (1993) 154.
[2] X. Li, Y. Liu, L. Fu, Carbon 46 (2008) 255.
[3] L.B. Adveeva, O.V. Goncharova, D.I. Kochubey, V.I. Zaikovskii, L.M. Plyasova, B.N. Novgorodov, Appl. Catal. A 141 (1996) 117.
[4] N.A. Kiselev, J. Sloan, D.N. Zakharov, E.F. Kukovitskii, J.L. Hutchison, J. Hammer, Carbon 36 (1998) 1149.
[5] Y. Wen, Z. Shen, Carbon 39 (2001) 2369.
[6] D.S. Bethune, C.H. Kiang, M.S. deVries, G. Gorman, R. Savoy, J. Vazquez, R. Beyers, Nature 363 (1993) 605.
[7] A. Thess, R. Lee, P. Nikolaev, H. Dai, P. Petit, J. Robert, C. Xu, Y.H. Lee, S.G. Kim, A.G. Rinzler, D.T. Colbert, G.E. Scuseria, D. Tomanek, J.E. Fisher, R.E. Smalley, Science 273 (1996) 483.
[8] Z.F. Ren, Z.P. Huang, J.W. Xu, J.H. Wang, P. Bush, M.P. Siegal, P.N. Provencio, Science 282 (1998) 1105.
[9] S. Fan, M.G. Chapline, N.R. Franklin, T.W. Tombler, A.M. Cassell, H. Dai, Science 283 (1999) 512.
[10] Y. Li, W. Kim, Y. Zhang, M. Rolandi, D. Wang, H. Dai, J. Phys. Chem. B 105 (2001) 11424.
[11] S. Sato, A. Kawabata, M. Nihei, Y. Awano, Chem. Phys. Lett. 382 (2003) 361.
[12] M.S. Dresselhaus, Nat. Mater. 3 (2004) 665.
[13] Q. Paula, G.N. Albert, G. David, T. Unto, J. Hua, T. Taku, G. Kestas, Carbon 44 (2006) 1581.
[14] E. Terrado, M. Redrado, E. Munõz, W.K. Maser, A.M. Benito, M.T. Martínez, Mater. Sci. Eng. C 26 (2006) 1185.
[15] M.M. Shaijumona, N. Bejoyb, S. Ramaprabhu, Appl. Surf. Sci. 242 (2005) 192.
[16] N.Q. Zhao, C.N. He, J. Alloy Compd. 428 (2007) 79.
[17] C. He, N. Zhao, X. Du, J. Ding, C. Shi, J. Li, Scr. Mater. 54 (2006) 689.
[18] R.T.K. Baker, M.A. Barber, P.S. Harris, F.S. Feates, R.J. Waite, J. Catal. 26 (1972) 51.
[19] R.T.K. Baker, P.S. Harris, R.B. Thomas, R.J. Waite, J. Catal. 30 (1973) 86.
[20] R.T. Yang, J.P. Chen, J. Catal. 115 (1989) 52.
[21] M. Tomellini, D. Gozzi, A. Latini, J. Phys. Chem. C 111 (2007) 3266.
[22] S. Helveg, C. López-Cartes, J. Sehested, P.L. Hansen, B.S. Clausen, J.R. Rostrup-Nielsen, F. Abild-Pedersen, J.K. Nørskov, Nature 427 (2004) 426.
[23] D. Gozzi, A. Latini, G. Capannelli, F. Canepa, M. Napoletano, M.R. Cimberle, M. Tropeano, J. Alloy Compd. 419 (2006) 32.
[24] D. Gozzi, A. Latini, M. Tomellini, J. Phys. Chem. C 113 (2009) 45.
[25] H. Terrones, T. Hayashi, M. Munoz-Navia, M. Terrones, Y.A. Kim, N. Grobert, et al., Chem. Phys. Lett. 343 (2001) 241.
[26] E.F. Kukovitsky, S.G. L'vov, N.A. Sainov, Chem. Phys. Lett. 317 (2000) 65.
[27] Ph. Buffat, J.-P. Borel, Phys. Rev. A 13 (1976) 2287.
[28] E. Flahaut, F. Agnoli, J. Sloan, C. OConnor, M.L.H. Green, Chem. Mater. 14 (2002) 2553.
[29] R.J. Nemanich, S.A.F. Solin, Phys. Rev. B: Condens. Matter Mater. Phys. 20 (1979) 392.